

Observation of isomeric decays and the high spin states in doubly-odd ^{208}Fr

D. Kanjilal^a, S. Bhattacharya^{a,b}, A. Goswami^a, R. Kshetri^a, R. Raut^a, S. Saha^{*,a,b}, R. K. Bhowmik^c, J. Gehlot^c, S. Muralithar^c, R. P. Singh^c, G. Jnaneswari^d, G. Mukherjee^e, B. Mukherjee^f

^a*Nuclear and Atomic Physics Division, Saha Institute of Nuclear Physics, Kolkata 700064, India*

^b*Centre for Astro-Particle Physics, Saha Institute of Nuclear Physics, Kolkata 700064, India*

^c*Inter University Accelerator Centre, New Delhi 110067, India*

^d*Department of Physics, Andhra University, Vishakhapatnam 530003, India*

^e*Variable Energy Cyclotron Centre, Kolkata 700064, India*

^f*Department of Physics, Visva Bharati, Santiniketan 731235, India*

Abstract

Neutron deficient isotopes of Francium ($Z=87$, $N \sim 121 - 123$) as excited nuclei were produced in the fusion-evaporation reaction: $^{197}\text{Au} (^{16}\text{O}, xn) ^{213-x}\text{Fr}$ at 100 MeV. The γ rays from the residues were observed through the high sensitivity Germanium Clover detector array INGA. The decay of the high spin states and the isomeric states of the doubly-odd ^{208}Fr nuclei, identified from the known sequence of ground state transitions, were observed. The half lives of the $E_\gamma = 194(2)$ keV isomeric transition, known from earlier observations, was measured to be $T_{1/2} = 233(18)$ ns. A second isomeric transition at $E_\gamma = 383(2)$ keV and $T_{1/2} = 33(7)$ ns was also found. The measured half lives were compared with the corresponding single particle estimates, based on a the level scheme obtained from the experiment.

Key words:

PACS: 21.10.Tg, 23.20.Lv, 23.35.+g, 27.80.w

1. Introduction

Investigation on the nuclear structure of the trans-Lead neutron deficient nuclei ($Z > 82$, $N < 126$) have attracted much attention in recent years[1, 2, 3]. For many of these nuclei, only the ground state spin and parity are known from their g -factor/magnetic moment measurements, and perhaps a few low lying excited states are observed so far. The major difficulties in populating the high spin states in these nuclei are: a) very low cross sections for the formation of evaporation residues (ER), and b) very high probability of fission, which removes flux from the ER channel and prevents the excited nucleus from sustaining large angular momenta needed to populate the high spin states.

Experimental investigation of the high spin states of quite a few trans-Lead neutron deficient nuclei have been of interest recently. A series of investigations on the $^{211-214}\text{Fr}$ isotopes[4, 5] showed that the structure can be interpreted in terms of the shell model states, and the excited states reveal an interplay between the protons in the $(1h_{9/2}, 2f_{7/2}, 1i_{13/2})$ states and the neutron holes in the $(2f_{5/2}, 3p_{3/2}, 1i_{13/2})$ orbitals, or the neutrons promoted to the $(2g_{9/2}, 1i_{11/2}, 1j_{15/2})$ high spin orbitals by core excitation, leading to the generation of high spin states. One of the major interests in the spectroscopic investigation of these nuclei is the role played by the $i_{13/2}$ shell in creating isomeric levels which decay through transitions of higher multipolarity or are hindered by the close proximity of the levels below.

A few spectroscopic investigations on the proton rich lighter Francium isotopes have been made recently. While a complete study of the $^{205-207}\text{Fr}$ nuclei[1], using Gammasphere and the HERCULES II array for filtering out the evaporation residues from the fission background, revealed the existence of shears band in ^{207}Fr ($N = 120$), investigations on the $^{208-210}\text{Fr}$ nuclei[2, 3] have resulted in contradictory conclusions. Spectroscopic studies made using the YRAST BALL array, comprising six Compton suppressed Clover HPGe detectors[2], coupled to the SASSYER recoil separator[6] for selecting the evaporation residues had concluded that the pair of intense gamma

*Corresponding author

Email address: satyajit.saha@saha.ac.in (S. Saha)

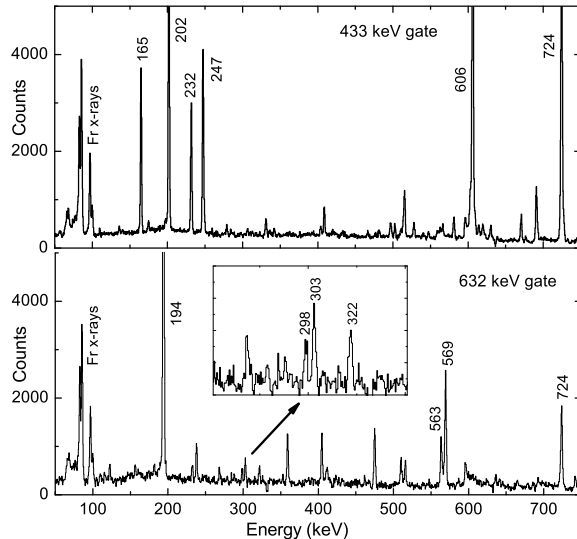


Figure 1: A few gated spectra of the Fr isotopes.

rays of 632 keV (ground state transition) and 194 keV (isomeric transition) belong to ^{209}Fr . The half life of the isomeric transition was measured to be 446(14) ns. At the same time, another independent study of isomeric decay of proton rich nuclei produced by projectile fragmentation reaction of ^{238}U beam at 900 MeV/u on ^9Be target at the Fragment Recoil Separator (FRS) facility of GSI, Darmstadt, Germany had assigned the same pair of gamma rays to ^{208}Fr [3]. Clean isotopic and isobaric resolution of nuclei, which have low lying isomers with half lives $\gtrsim 100$ ns, are routinely achieved using this facility[7]. Half life of the 194 keV isomeric transition was reported to be ~ 200 ns, though the prompt transitions above the isomer could not be observed because of experimental constraints. This paper reports investigation of the isomeric transitions in ^{208}Fr , along with the high spin states above the isomers. It is noteworthy to report here that at the time of final phase of data analysis and preparation of the manuscript, a paper on assignments of levels in ^{208}Fr was published by G. D. Dracoulis et al.[8]. The differences in our methods, the results of observations on the isomeric transitions, new γ transitions over and above those reported therein, and the basis for our assignments of the isomeric transitions to ^{208}Fr are highlighted in this paper.

2. Experiment and data analysis

The experiment to produce ^{208}Fr was carried out at the Inter-University Accelerator Centre (IUAC), New Delhi. The Fr isotopes were produced by bombarding a 3.5 mg.cm^{-2} self-supporting Gold (99.95% purity) target with ^{16}O beam at 88, 94 and 100 MeV. The nuclei of interest were produced as evaporation residues (ER) through $(^{16}\text{O}, xn\gamma)$ reactions. The target thickness was chosen on the basis of energy loss calculations based on SRIM2003[9] to stop more than 90% of the ER within the target, and allow most of the fission fragments to fly away from it. Estimation of cross sections, angular distributions of the evaporation residues (ER) and the fission yield were done using the code PACE[10]. Based on these calculations, $\sim 60 - 80$ % of the fusion products at these bombarding energies undergo fission, which causes a huge background. Therefore, an effective filter to clean up the spectra, and / or good statistics are essential for extraction of meaningful results, as were done recently[1]. In the absence of such filters, use of large gamma detector arrays with high resolving power, good efficiencies for $\gamma\gamma$ and $\gamma\gamma\gamma$ coincidence events, along with additional measurements of excitation functions from in-beam and off-beam measurements yielding consistent results, have been utilized in our attempt to resolve the ambiguity.

The γ -rays produced were detected by the Indian National Gamma Array (INGA) consisting of 18 Compton suppressed Clover Germanium detectors placed around the target[11] at the INGA-HYRA beam line of the IUAC, New Delhi. Four Clover detectors were placed at 57° , six at 90° , four at 123° , and four at 148° for facilitating measurement of directional correlation from oriented states (DCO) ratios. The linear signals, along with the anti-coincidence logic and the trigger signals, were processed through the indigenously developed Clover electronics modules dedicated for the INGA set-up[12]. Since the measurement of half lives of the isomeric states is crucial for

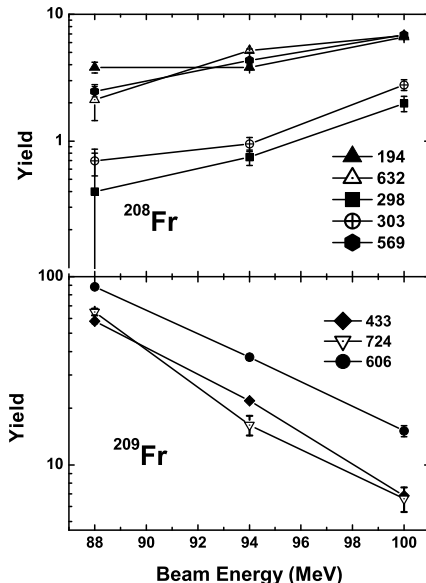


Figure 2: Excitation functions measured by tagging on the strong gamma transitions.

the experiment, time to digital converters (TDC) were used with stop signals from the individual Clover units and common start signal from the master trigger which can be chosen to select 2-fold or higher fold events. Range of the TDC was set to 400 ns for the exclusion of delayed γ -rays possibly coming from α - and β decays. Altogether 315×10^6 two-fold and 48×10^6 three-fold coincidences were recorded in ~ 50 hours at 100 MeV beam energy, and $\sim 20\%$ of above numbers were obtained at 88 and 94 MeV. In order to identify and measure the yield of the ER nuclei from their known α - and β -decay modes, data were taken in the multiscaling mode during the beam-off condition between the runs. All the on-line and off-line data were collected using the CAMAC-based CANDLE data acquisition system[13], and were analysed off-line using CANDLE, INGASORT[14] and RADWARE[15] analysis softwares.

Data analyses were done in several steps. For the excitation function measurements, $\gamma\gamma$ coincidence matrices were generated from the 2-fold data collected at the three different energies. Yields for the intense γ -rays, normalized by the current integrator readings recorded at the beam dump during the excitation function runs, were obtained from the Francium K_α and K_β x-ray gated projections of the symmetrized matrices for each energy. The gated spectra are shown in the Fig. 1, where the intense γ -rays of ^{208}Fr and ^{209}Fr are indicated. The 724 keV γ -ray is present in both the nuclei, and hence could not be resolved in the experiment. Since its intensity is stronger in the decay of ^{209}Fr levels, the excitation function shows the energy dependence typical of ^{209}Fr . The trends of the excitation functions graphs for ^{208}Fr and ^{209}Fr , shown in the Fig. 2 are comparable to that predicted from the PACE calculations, though it overestimates the ^{208}Fr yield and underestimates the ^{209}Fr yield at 100 MeV. The ^{210}Fr yield could not be measured even at the two lower energies as the corresponding characteristic γ -rays are not known.

The relative yields of the Fr isotopes ($A = 208 - 210$) at the three different energies were also obtained from the radioactive decay runs taken in the beam-off condition. The time stamps in the list data blocks were used to generate the time marker. The E_γ vs. time matrices were generated using the CANDLE analysis software from which, the E_γ spectra at different time windows were generated. The decay curves for the intense characteristic γ -rays belonging to the decay branches of these nuclei were obtained. A few decay curves are shown in the Fig. 3. The ERs decay via their well known α - and β -decay branches, with half lives which are well documented for these nuclei. The half lives $T_{1/2}$, obtained by fitting the equation: $n = n_0 \exp(-0.693 t/T_{1/2})$ for different decay branches observed in this experiment, are enlisted in the Table 1. The results show reasonably good agreement with the reference values quoted in the NNDC database[16, 17, 18, 19, 20, 21]. Relative yields of different ERs at the beginning of beam-off runs, were extracted from the fitted n_0 values, measured half lives and the branching fractions of the different decay branches. The relative yields, obtained from our data for the Fr isotopes, are shown in the Table 1. The major contribution to the uncertainties ($\lesssim 5\%$) quoted in the relative yields is from the fluctuation

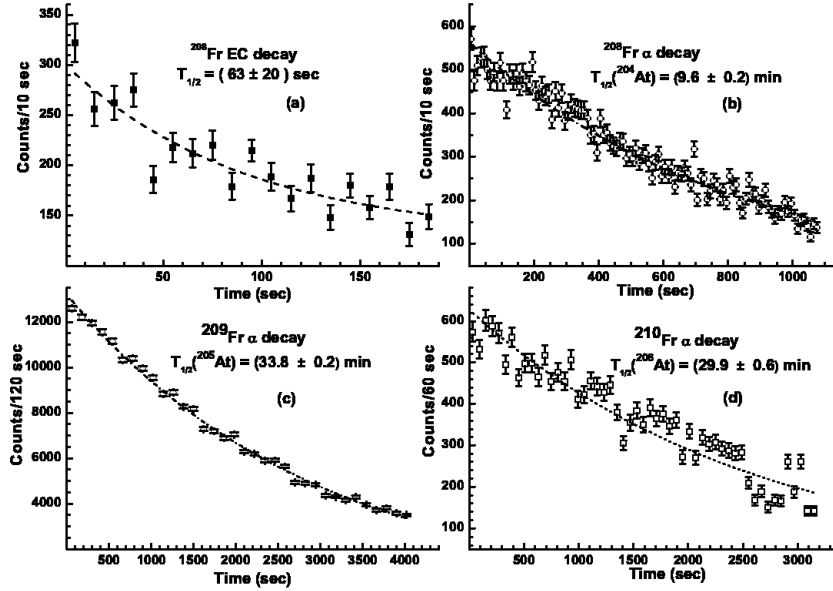


Figure 3: Offline decay plots of various isotopes used for extracting the yield ratio of the Francium evaporation residues.

in the beam current before the beginning of the beam-off runs, which were monitored during the analysis, and the rest from the exponential fit to the data. The results are in reasonable agreement with the measured excitation functions of Fig. 2, which agrees with the assignment of the 826 keV isomeric level and the corresponding gamma transitions to ^{208}Fr , rather than to ^{209}Fr [2], in agreement with the conclusions of Refs. [3, 8].

From the online data taken at 100 MeV beam energy, the $\gamma - \gamma$ matrices, Francium X -ray gated $\gamma\gamma$ matrices, the prompt and the delayed $\gamma\gamma$ matrices and the γ -gated $\gamma\Delta T$ matrices were constructed for establishing the level scheme and resolving the isomeric transitions. From the first two sets of matrices and by gating on the strongest 632 keV ground state transition and the intense 194 keV transition, the γ -transitions belonging to ^{208}Fr were clearly established. These transitions, observed at 100 MeV beam energy, are shown in the Table 2. The relative intensities given in the table were obtained from the 632 keV gated spectra. Because of the existence of low lying isomer with half lives $\sim 200 - 400$ ns, and also due to the large internal conversion of some of the levels, the intensity balance across the isomeric levels could only approximately be done. The observed γ -rays and their relative intensities match reasonably well with those obtained recently by Dracoulis et al.[8]. However, quite a few additional γ -transitions were observed and indicated in the table. A directional correlation of oriented nuclei

Table 1: Half lives and relative yields of Fr isotopes from the off-line decay runs. Percent figures within brackets in col. 2 are the branching fractions. The characteristic γ -transitions E_γ (col. 5), monitored for decay analysis, are the strongest lines in the corresponding daughter nuclei. The yields given are the extracted relative yields at each beam energy.

ER	Decay branch	$T_{1/2}$	$T_{1/2}$ (This expt)	E_γ (keV)	Yield (88 MeV)	Yield (94 MeV)	Yield (100 MeV)
^{208}Fr	$^{208}\text{Fr} \rightarrow ^{208}\text{Rn}$ (11%)	59.1(3) sec[16]	63(20) sec	635.8			
	$^{208}\text{Fr} \rightarrow ^{204}\text{At}$ (89%)						
	$^{204}\text{At} \rightarrow ^{204}\text{Po}$ (96%)	9.2(2) min[17]	9.6(2) min	516.3	0	0.14(1)	0.46(8)
^{209}Fr	$^{209}\text{Fr} \rightarrow ^{209}\text{Rn}$ (11%)	50.0(3) sec[18]					
	$^{209}\text{Fr} \rightarrow ^{205}\text{At}$ (89%)						
	$^{205}\text{At} \rightarrow ^{205}\text{Po}$ (90%)	26.9(8) min[19]	33.8(2) min	719.3	1.0(2)	1.00(5)	1.0(3)
^{210}Fr	$^{210}\text{Fr} \rightarrow ^{210}\text{Rn}$ (40%)	3.18(6) min[20]	3.4(2) min	643.8			
	$^{210}\text{Fr} \rightarrow ^{206}\text{At}$ (60%)						
	$^{206}\text{At} \rightarrow ^{206}\text{Po}$ (99%)	30.0(8) min[21]	29.9(6) min	700.7	0.35(5)	0.18(1)	0.37(7)

Table 2: Intensities and DCO ratios of the γ -rays of ^{208}Fr at 100 MeV beam energy. Intensities are normalized relative to the 632 keV ground state transition. Newly found γ -transitions in this experiment are indicated by ^a. For the DCO ratios, the gating transitions are indicated in col. 6. Multipolarity of the gating transitions are indicated in brackets and the multipolarity assignments are shown in col. 7.

E_γ (keV)	I_γ	E_i (keV)	E_f (keV)	R_{DCO}	E_γ (gate) (keV)	Multipolarity
110.0(20) ^a	11.00(45)	4077	3967			
115.8(20) ^a	7.58(31)	3967	3851			
122.7(18) ^a	17.9(13)	3851	3728			
123.2(14) ^a	8.6(10)	2262	2139			
150.2(17) ^a	8.3(17)	3856	3706			
156.4(17) ^a	13.4(18)	2139	1983			
160.1(17)	9.9(25)	4070	3910	1.26(59)	303(M1)	M1
181.8(18) ^a	11.6(19)	3910	3728	1.20(39)	303(M1)	M1
194.1(18)	818(12)	826	632	0.99(6)	632(E2)	E1 ($9^- \rightarrow 9^+$)
209.7(19) ^a	8.70(79)	2763	2553	~ 0.5	303(M1)	E2
232.4(18)	15.9(13)	4325	4093	1.93(80)	569(E2)	M1
238.2(18)	38.8(16)	4093	3855	1.74(32)	569(E2)	M1
268.5(14) ^a	15.4(20)	1983	1715			
284.6(15) ^a	5.0(16)	3048	2763	~ 0.5	303(M1)	E2
288.1(18)	11.39(4)	2246	1958	~ 0.5	569(E2)	M1
290.9(15) ^a	3.8(13)	2553	2262	~ 0.5	303(M1)	E2
298.8(19)	17.1(28)	2133	1834	1.04(13)	303(M1)	M1
303.1(19)	26.8(35)	1512	1209	2.1(6)	632(E2)	M1
313.1(17) ^a	3.9(12)	3728	3415	~ 0.5	303(M1)	(E2)
321.8(22)	24.8(12)	1834	1512	1.02(18)	303(M1)	M1
359.3(21)	67.6(41)	1715	1356	1.03(21)	632(E2)	E2
365.4(16) ^a	4.5(12)	2633	2268			
382.9(18) ^a	7.13(90)	1209	826	0.60(17)	322(M1)	E2
404.8(19)	64.9(39)	1800	1395	0.92(12)	569(E2)	M1/E1 ($11 \rightarrow 11$)
410.7(13) ^a	8.45(76)	3415	3004	~ 0.5	303(M1)	(E2)
428.3(15) ^a	7.0(13)	2262	1834	0.50(34)	303(M1)	E2
467.8(21) ^a	9.61(41)	2268	1800	0.8(4)	405(M1/E1)	M1/E1 ($11 \rightarrow 12$)
498.6(13) ^a	4.5(12)	3706	3207			
510.2(22)	40.6(33)	3190	2680	~ 2	569(E2)	M1
563.5(24)	88.4(45)	1958	1395	1.85(44)	632(E2)	M1
566.2(24) ^a	27.1(38)	5487	4921	0.44(17)	563(M1)	E2
569.4(24)	197.7(62)	1395	826	0.89(9)	632(E2)	E2
596.2(24) ^a	38.5(47)	4921	4325	2.0(8)	632(E2)	M1
603.6(26) ^a	12.3(26)	3207	2603			
632.2(19)	1000	632	0			E2
645.3(19) ^a	8.9(31)	2603	1958	0.6(4)	563 (M1)	(E1/M1) ($12 \rightarrow 12$)
665.1(20) ^a	11.7(47)	3855	3190	1.05(37)	563(M1)	M1
721.6(23) ^a	21.0(38)	2680	1958	1.0(6)	563(M1)	M1
723.9(23)	160.30(46)	1356	632	1.14(11)	632(E2)	E2
742.0(23)	32.2(13)	3004	2262	0.56(23)	303(M1)	E2
774.6(18)	5.28(2)	2169	1395	~ 1	569(E2)	(E2)
880.2(16)	7.26(2)	2680	1800	~ 1	569(E2)	(E2)
955.8(16) ^a	3.6(11)	4004	3048	0.49(24)	303(M1)	(E2)

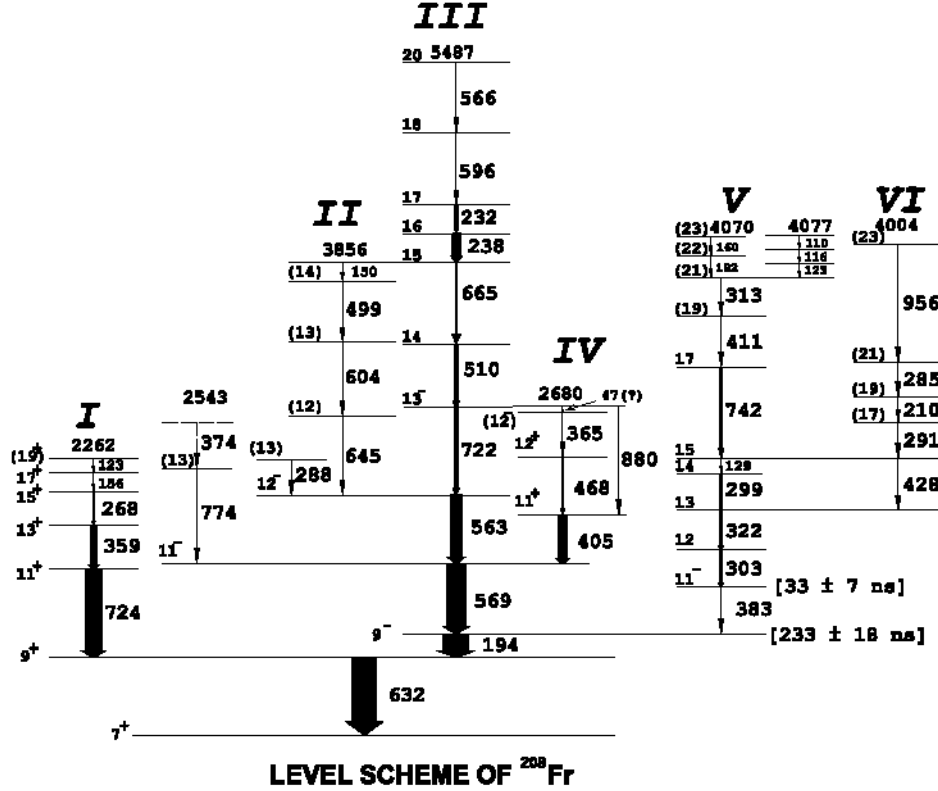


Figure 4: Level scheme of ^{208}Fr obtained from the present work. Transitions which were not observed but necessary to fit the level scheme are indicated by ?. The dotted transitions are observed in the previous work[8], but not in this work.

(DCO) analysis was also performed with the data taken at $(90^\circ, 148^\circ)$ and $(90^\circ, 123^\circ)$ angle pairs. The gating transitions and their multiplicities used for DCO ratio calculations are shown in the Table 2. These assignments match with those obtained in Ref. [8].

Based on the intensity correlations obtained from our gated spectra, and also from the DCO ratio measurements, the level scheme for ^{208}Fr was established as shown in the Figure 4. Apart from one sequence of transitions (I) passing through 359 and 724 keV, which directly feeds the 632 keV first excited state, two major sequences (III and V) and three minor sequences (II, IV and VI) of transitions, which pass through the isomeric 826 keV level, have been observed. A few relevant gated spectra are shown in the Figs. 5 and 6. Out of these, three sequences (II, III and IV) of transitions pass through the strong 569 keV transition, and two (V and VI) through the sequence of 303 and 322 keV transitions. In all the major sequences, ordering of the transitions are cross-checked by intensity correlations and also by reverse gating.

About 25 new transitions, over and above those observed by Dracoulis et al.[8], were found, as noted in the Table 2. The 722 keV transition in sequence III falls on the tail of the much stronger 724 keV transition of sequence I, and could only be observed in the 238 and 569 keV gates, as shown in the Fig. 6, except for a small contamination at 725 keV in the 569 keV gate, possibly coming from ^{198}Au produced by neutron transfer reaction. The 725 keV contamination was also present in the 194 keV gated spectrum for the same reason mentioned above. The 724 keV contamination line was not found in the 563 keV gate. The contamination from the 724 keV transition is much more severe as it also belongs to ^{209}Fr . Similarly, the 510 keV γ -ray is also a new line, which was observed consistently in the coincident gates of sequence III transitions. It was placed in the level scheme just above the 722 keV transition, based on the observed intensities in various forward and reverse gates. The 665-510-722 keV sequence in III is bypassed by the 150-499-604-645 keV sequence II transitions which is evident from the 645 keV gated spectrum of Fig. 5 b. The 665 keV and the 150 keV transitions are weak in intensity and allow only an approximate intensity balance. The sequence I was known up to 359 keV[8], which was extended with the 123-156-268 keV transitions observed by overlapping the 632,724 and 359 keV gated spectra (see Fig. 5a). The sequence

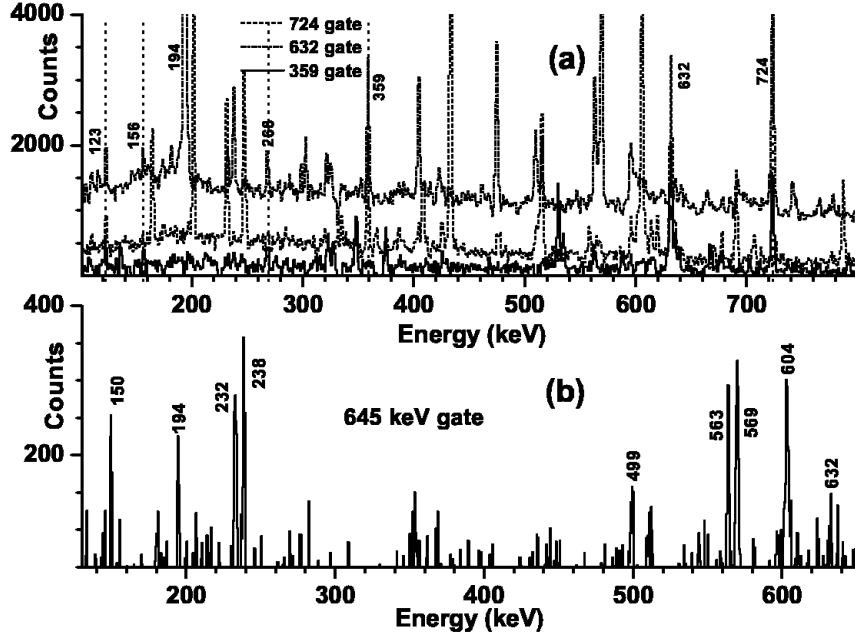


Figure 5: (a) Overlap of the 359, 632 and 724 keV gated spectra manifesting the sequence I transitions above the 1750 keV level. (b) The 645 keV gated spectrum for the sequence II transitions.

IV transitions pass through 569 keV but they bypass the 563 keV and 722 keV transitions and hence were placed accordingly. The 880 keV transition, which was also shown in Ref. [8], was absent in 365 and 468 keV gates, but present in the 405 keV gate. Hence it was placed to directly feed the 1800 keV level. By matching the sum energies of the relevant transitions in IV, a 47 keV transition was placed just below the 2680 keV level. This, perhaps, could not be identified due to the absorbers placed in front of the Clover detectors.

For the sequence V and VI, several new transitions were found and the relative ordering was modified over the level scheme shown in Ref. [8]. 210, 284, 291 and 956 keV lines were observed for the first time in the 299, 303 and 322 keV gates (see Fig. 6a), but absent from the 742 keV gate. This makes the placement of 742 keV above the 299-303-322 keV sequence. Further, the 428 keV line was present in the 303, 322 and 742 keV gates but absent in the 299 keV gate. This was also confirmed by reverse gating on 428 keV. The 129 keV line, though weak possibly because of internal conversion, was present in 299, 303 and 322 keV gates but absent in the 428 keV gate, which makes its placement sequential to 299 keV but parallel to 428 keV. The γ -rays coming from the levels above 3004 keV in sequence V were observed for the first time, except for the 160 keV transition which has already been reported[8]. A new 383 keV feeding transition to 826 keV level along the sequence V was found. Justification for its placement is given below.

One of the major point of controversy is the life time of the 826 keV isomeric level, which has been measured by several workers[2, 3, 8], and the existence of other isomers in ^{208}Fr . A systematic search for isomeric transitions were done from our data and the half lives were extracted. The ΔT spectral measurements covered a ± 400 ns TDC range, but an useful range of ~ 500 ns could be utilized due to delay matching of the detector array. Typical ΔT spectra gated by 632 keV are shown in the Fig. 7. From the 194 keV and 632 keV γ -gated $\gamma\Delta T$ coincidence matrices, we have projected the gated ΔT spectra for the 569 keV, 563 keV, 299 keV, 303 keV, 322 keV and 742 keV gated transitions. The ΔT spectra for the first two gated transitions are found to be similar in nature. This clearly establishes the fact that 563 and 569 keV transitions are in sequence and above the 826 keV isomeric level. The combined ΔT spectrum for the 563 + 569 keV as start and 632 keV as stop are shown in the Fig. 7(a). However, the ΔT spectra for the 299, 303, 322 and 742 keV as start and 194 or 632 keV as stop, though similar in nature among themselves, differ significantly from the previous ones (see Fig. 7(a,d)) in that the exponential decay is much faster indicating the existence of another faster isomeric transition above the 826 keV level. The gated ΔT spectra obtained for the gates between the pairs of γ -rays among the 299, 303, 322 and 742 keV, the 563 and 569 keV pair of γ -rays showed their prompt nature. By comparing the prompt and delayed gated spectra, taken

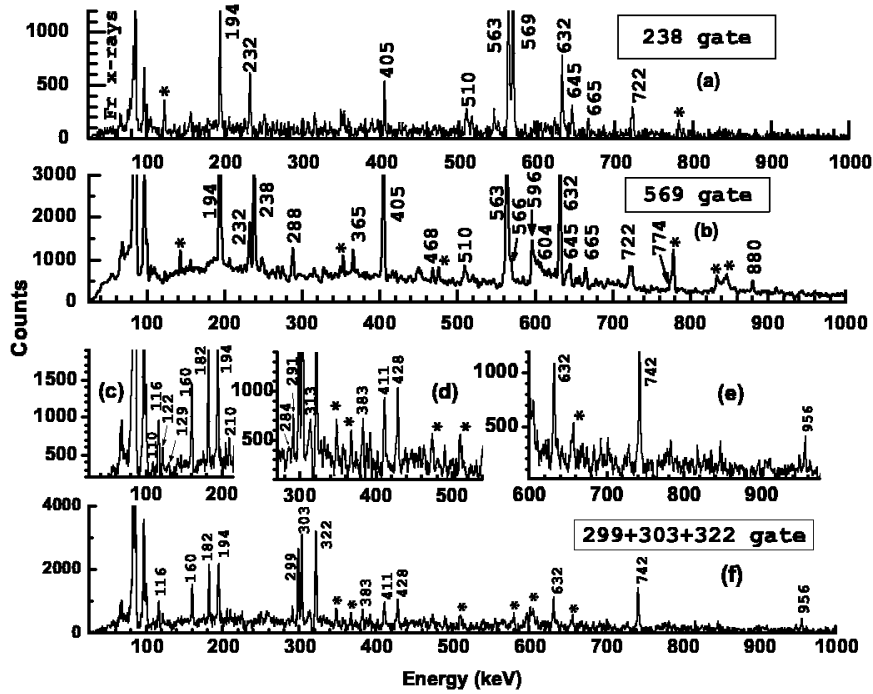


Figure 6: A few relevant gated spectra of ^{208}Fr . Gating transitions are indicated in the figures. Contamination lines are indicated by *. Plots in (c) to (e) are zoomed plots of the spectra shown in (f), to bring out the weak transitions noted in the experiment.

for the sequence V transitions mentioned above, a new but weak 383 keV isomeric transition was found and it was placed just above the 826 keV level along the sequence V.

The half life of the 826 keV isomeric level was extracted by fitting exponential decay function to the ΔT spectra, shown in the Fig. 7(c). The results are given in the Table 3. Half life of 233 ± 18 ns was obtained, which is consistent with the result ~ 200 ns quoted in Ref. [3]. However, the result differs from that obtained recently by Dracoulis et al.[8]. Half life of the 1209 keV isomeric level was extracted from the ΔT spectra of Fig. 7(b), in a similar way. The result obtained is: 27.6 ± 3.4 ns. The same half life was extracted independently from the ΔT spectrum shown in Fig. 7(d), using two exponential decay fit and the measured half life of the 826 keV isomer mentioned above. The results were mutually consistent and the average of the two measurements is quoted in Table 3.

3. Interpretation of results

The difference in the measured values of the 826 keV isomer half life could not be explained. One of the drawback of the present measurement is the restricted range of ΔT . This could not be avoided in the experimental set up of the INGA array, which was optimized for prompt γ -spectroscopy. To find out the correctness of the present technique, half lives have been extracted for a number of isomeric transitions already known in several nuclei produced in our in-beam experiment. These are listed in the Table 3. The isomer half lives spanned from ~ 150 ns to ~ 600 ns. The results are found to be in good agreement with the earlier measurements, within the quoted uncertainties. The half life for ^{206}At was also reported in Ref. [8] as 813 ± 21 ns, which is almost twice that obtained earlier[23]. While the probable cause of this difference was cited as due to the restricted TDC range ± 300 ns in the previous work, our result does not seem to agree with this conclusion. We get results which are consistent with earlier measurements, though the uncertainties are larger in case of larger half lives (eg. ^{208}Rn [22]). The restricted range of TDC would result in poor statistics for fitting data, with consequent larger error bars, as manifested in our results.

The results of DCO ratio measurements are enlisted in the Table 2. These measurements are pivoted on the $E2$ assignment of the 632 keV ground state transition, which follows from the systematics in the neighbouring nuclei, including Francium isotopes. Based on our DCO results, $\Delta J = 0$ $E1$ character was assigned to the 194 keV isomeric

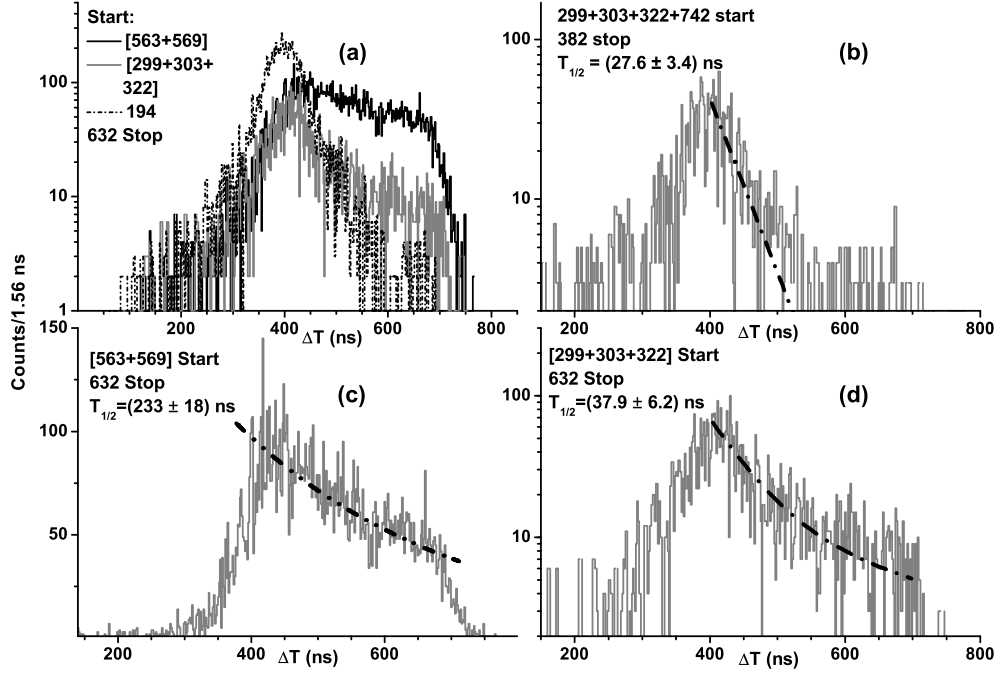


Figure 7: Different ΔT spectra used to search for and measure the half lives of the isomeric transitions in ^{208}Fr .

Table 3: Half lives of isomeric levels of different nuclei produced in the experiment.

Nucl.	Level	E_γ	ML	$T_{1/2}(\text{ns})$	$T_{1/2}(\text{ns})$
	(keV)	(keV)		(This expt)	(Earlier)
^{208}Fr	826	194.1	$E1$	233(18)	432(11)[8] ~ 200 [3]
^{208}Fr	1209	382.9	$E2$	33(7)	
^{208}Rn	1828	88.7	$E2$	590(144)	509(14)[22]
^{206}At	807	121.6	$E1$	377(44)	410(80)[23] 813(21)[8]
^{204}Po	1639	12.1	$E2$	161(4)	158(2)[24]

transition. The same transition was assigned $E1(10^- \rightarrow 9^+)$ in Ref. [8]. However, both the J^π assignments arise from the same $\pi(1h_{9/2})^5 \otimes \nu(1i_{13/2})^{-1}$ configuration, with the only difference that the 9^- isomeric level would be placed higher than a 10^- state, as evident from the spin multiplets observed in ^{208}Bi from the neutron pick-up reactions[25]. The 11^- state, arising out of the same configuration, is assigned to the next 1209 keV level, which is also an isomeric level decaying by 383 keV $E2$ transition. Based on the measured half life and the estimated internal conversion coefficient of 0.0723(11)[26], single particle strength of 0.0264(12) W. u. was obtained. For the isomeric transition of the 826 keV 9^- level, internal conversion coefficient of 0.0947(14) was estimated, and the corresponding single particle strength was obtained as $1.06(8) \times 10^{-7}$ W. u. Similar results for the $E1$, $M1$, $E2$ and $M2$ isomeric transitions are obtained in trans-Lead nuclei(eg. ^{208}Rn [22]) in this mass region.

In the level scheme shown in Fig. 4, the series of levels from 632 keV (7^+) to 1983 keV (15^+) along sequence I arise from the $\pi(1h_{9/2})^5 \otimes \nu(2f_{5/2})^{-1}$ with proton excitations of higher seniority leading to the generation of angular momenta. This is clear from the connecting sequence of $E2$ transitions. The maximum angular momentum generated from proton excitation in this case is $25/2$, which leads to maximum $J^\pi = 15^+$ for the given configuration. The 123 and 156 keV transitions above the 1983 keV level could be of $E2$ nature, though our data is inadequate to make a definite conclusion.

The sequence II transitions, observed for the first time, are weak in intensity but they are fitted into the level scheme from the matched sequence of γ -ray energies, coincidence conditions and intensities. However, the spin assignments of only the 2603 keV level could be done from the DCO ratio for the 645 keV transition by gating on 563 keV $M1$ transition. This could be a stretched $E2$ transition or a $\Delta J = 0$ $M1$ transition, but the latter assignment was adopted to fix the spins of the level sequence. The 604 keV, 499 keV and 150 keV transitions appear to be $M1$ though it cannot be confirmed from our data. Sequence III transitions extend to the highest excitation energy of ^{208}Fr in this experiment. It starts from the 1395 keV 11^- level which is connected by 569 keV $E2$ transition to the 826 keV 9^- level. This sequence is likely to arise from the $\pi(1h_{9/2})^4(2f_{7/2}) \otimes \nu(1i_{13/2})^{-1}$ configuration which leads to the highest spin of 22^- , and are connected by a series of $M1$ transitions. Though we could extend up to 20^- level, the absence of 19^- level is possibly because of the fact that it is pushed down by the residual proton particle neutron hole repulsive interaction, from where gamma transitions are hindered. A detailed shell model calculation will be needed to make a definite conclusion in this regard.

The low lying transitions of the sequences V and VI, extending up to 2763 keV $J = 19$ level can be formed by $\pi(1h_{9/2})^5 \otimes \nu(1i_{13/2})^{-1}$ configuration through proton excitation. However, levels above 19^- along sequence VI, built on proton excitation to the maximum proton spin of $25/2$, are due to neutron hole excitation arising from $\nu(2f_{5/2})^{-2}1i_{13/2}^{-1}$, leading up to the maximum $J^\pi = 23^-$ level observed. The series of $E2$ transitions above the 2262 keV 15^- level along the sequence V can be between levels generated by $\pi(1h_{9/2})^4(1i_{13/2}) \otimes \nu(2f_{5/2})^{-1}$, which leads to a maximum $J^\pi = 21^-$. The levels above it are connected by $M1$ transitions which are probably generated by a different configuration. A better statistics and / or higher resolving power of the array will be needed to extend the level scheme further.

4. Conclusion

The level scheme of ^{208}Fr was modified over the existing level scheme, and extended up to $\sim 23\hbar$ and ~ 5.5 MeV excitation energy using a high resolving power Clover detector array. A number of new γ -transitions were observed and their DCO ratios were measured. Based on search for isomeric transitions from the data using the tagged $\gamma\gamma$ time difference technique, the half lives of several isomeric transitions in ^{208}Fr and in a few neighbouring nuclei produced as ER in the experiment were measured. The results agree reasonably well with the previously known half lives. The half life of the known 194 keV isomeric transition in ^{208}Fr was found to differ from the previously reported value. A new isomeric $E2$ transition was obtained and its half life was measured. The Weisskopf estimate of the single particle strength of the associated isomeric levels reveal similarity with the previous estimates in the neighbouring nuclei. From the shell model based interpretation of the level scheme, it is clear that the majority of the excited states are caused by $1h_{9/2}$ proton excitations, and neutron hole excitations predominantly in $2f_{5/2}$ and $1i_{13/2}$ shells. The importance of $1i_{13/2}$ neutron hole in generating the isomeric levels is clear from the present data. It may be noted that though we have observed only two isomer levels, there can be a few more such levels which could not be observed due to limited statistics in our data. A pulsed beam based experiment, coupled with such a high resolving power array will be needed to extend the study further.

5. Acknowledgement

We are grateful to all the colleagues of the INGA collaboration for their help during the experiment. Smooth running of the 16UD Pelletron accelerator and the INGA detector array at the IUAC, New Delhi by the staff therein are gratefully acknowledged.

References

- [1] D. J. Hartley et al. , Phys. Rev. C **78**, 054319 (2008).
- [2] D. A. Mayer et al. , Phys. Rev. C **73**, 024307 (2006).
- [3] Zs. Podolyak et al. , AIP Conf Proc **831**, 114 (2006).
- [4] A. P. Byrne, G. D. Dracoulis, C. Fahlander, H. Hübel, and A. R. Poletti, A. E. Stuchbery, J. Gerl, R. F. Davie, and S. J. Poletti, Nucl. Phys. **A** 448, 137 (1986).
- [5] A. P. Byrne, G. J. Lane, G. D. Dracoulis, B. Fabricius, T. Kibédi, A. E. Stuchbery, A. M. Baxter, and K. J. Schiffer, Nucl. Phys. **A** 567, 445 (1994).
- [6] J. J. Ressler et al. , Nucl. Instr. and Meth. B **204**, 141 (2003).
- [7] H. Geissel et al. , Nucl. Instr. and Meth. B **70**, 286 (1992).
- [8] G. D. Dracoulis, P. M. Davidson, G. J. Lane, A. P. Byrne, T. Kibédi, P. Nieminen, A. N. Wilson, and H. Watanabe, Euro. Phys. Jour. A **40**, 127 (2009).
- [9] James F. Ziegler, Nucl. Instr. Meth. **B** **219**, 1027 (2004).
- [10] A. Gavron, Phys. Rev. C **21**, 230 (1980).
- [11] S. Muralithar, et al., DAE Symp. on Nucl. Phys. **52**, 595 (2007).
- [12] S. Venkataramanan, et al., DAE Symp. on Nucl. Phys. **45B**, 424 (2002).
- [13] E. T. Subramaniam, Kusum Rani, B. P. Ajith Kumar and R. K. Bhowmik, Rev. Sci. Instr. **77**, 096102 (2006).
- [14] R. K. Bhowmik, S. Muralithar and R. P. Singh, DAE Symp. on Nucl. Phys. **44B**, 422 (2001).
- [15] D.C. Radford, Nucl. Instr. Meth. **A** **361**, 297 (1995).
- [16] M. J. Martin, Nucl. Data Sheets **108**, 1583 (2007).
- [17] M. R. Schmorak, Nucl. Data Sheets **72**, 409 (1994).
- [18] M. J. Martin, Nucl. Data Sheets **63**, 723 (1991).
- [19] F. G. Kondev, Nucl. Data Sheets **101**, 521 (2004).
- [20] E. Browne, Nucl. Data Sheets **99**, 649 (2003).
- [21] F. G. Kondev, Nucl. Data Sheets **109**, 1527 (2008).
- [22] W. J. Triggs, A. R. Poletti, G. D. Dracoulis, C. Fahlander, and A. P. Byrne, Nucl. Phys. **A** **395**, 274 (1983).
- [23] X. C. Feng, et al. , Eur. Phys. J. A **6**, 235 (1999).
- [24] V. Rahkonen and T. Lönnroth, Nucl. Phys. **A** **464**, 349 (1989).
- [25] G. M. Crawley, E. Kashy, W. Lanford, and H. G. Blosser, Phys. Rev. C **8**, 2477 (1973).
- [26] T. Kibédi, T.W. Burrows, M.B. Trzhaskovskaya, P.M. Davidson, C.W. Nestor Jr., Nucl. Instr. and Meth. **A** **589**, 202 (2008).